

Controlled Variation of Spacer Segment in Hyperbranched Polymers: From Densely Branched to Lightly Branched Systems

Girish Ch. Behera and S. Ramakrishnan*

Department of Inorganic and Physical Chemistry, Indian Institute of Science, Bangalore 560012, India

Received June 24, 2004; Revised Manuscript Received September 21, 2004

ABSTRACT: A series of hyperbranched polyethers containing different types (and lengths) of spacer segments that link the branch points were prepared by a solvent-free melt transesterification methodology. Three types of spacers, namely *n*-alkylene, cycloalkylene, and oxyethylene, were incorporated into the hyperbranched structures in order to examine the role of spacer length (and flexibility) on the relative compactness of the chain conformation as well as to study its effect on their T_g . The distinctive feature of this investigation is that the branching density (number of branch-points per unit volume) is varied in a controlled manner by utilizing AB_2 -type monomers that contain spacer segments of different lengths. GPC studies using a dual detector (RI-DV) system revealed that most of the polymers were of fairly high molecular weight, with M_w values ranging from 24 000 to 90 000. It is seen that as the branching density decreases, i.e., when the spacer segment length increases, the Mark–Howink exponent “ a ” increases; for instance, it increased from 0.37 for the polymer without a spacer to 0.54 in the case of the polymer having a 10-carbon spacer segment. This suggests that the relative compactness of the hyperbranched structures diminishes with increasing length of the spacer segment and might be expected to approach the behavior of linear macromolecules for even longer spacers. Furthermore, comparison of the molecular weights of several fractionated samples, determined by both the standard polystyrene calibration plot as well as by the universal calibration plot, reveals that the extent of molecular weight underestimation using the PS calibration becomes significant only at higher molecular weights. Thus, as seen in dendrimers, in hyperbranched polymers also compact structures are formed only beyond a certain molecular weight. The glass transition temperatures of the hyperbranched polymers were seen to decrease monotonically with increasing spacer length within each series, and hyperbranched structures with relatively flexible spacers exhibited lower T_g values when compared to ones with relatively rigid spacers of similar length.

Introduction

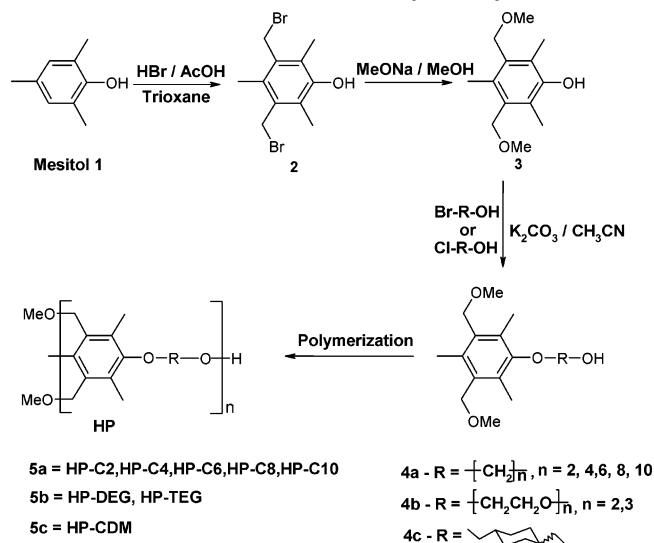
Hyperbranched polymers¹ represent a class of highly branched soluble macromolecules, which has witnessed growing attention during the past decade, and this has resulted in the development of several new and simpler synthetic approaches for their preparation. A large variety of hyperbranched structures have been prepared utilizing both the traditional self-condensation of simple AB_2 -type monomers and the more recent $A_2 + BB_2$ type polycondensation route and other similar methodologies.² Alternate approaches, such as the self-condensing vinyl polymerization³ and proton-transfer polymerization routes,⁴ have expanded the structural range of hyperbranched systems to encompass a much wider variety of polymer types. One of the important driving motivations for this sustained interest in hyperbranched polymers is that they possess a compact structure and have a large number of functional chain ends. Thus, despite the presence of significant structural imperfections, the simplicity of their preparation and their ability to mimic several properties exhibited by the structurally perfect dendrimeric analogues has led to a steady increase in the effort aimed at eliciting useful properties from highly branched polymers.¹

Despite this dramatic increase in the research efforts in this area, several aspects concerning the correlation of various molecular structural features and the physical properties of hyperbranched polymers remain poorly understood. One important question concerns the role of the linear spacer segment, which links the branch

points, in governing the physical properties of these macromolecules. It is apparent that a controlled variation of the length of spacer segment will result in a gradual change in the branching density—going from densely branching systems (for small spacer lengths) to lightly branched ones (for longer ones). One approach to vary the branching density in hyperbranched polymers is to utilize an $AB + AB_2$ type co-polycondensation approach, wherein the extent of branching can be controlled by varying the comonomer composition. While the branching density can be controlled over a very wide range using this approach, the relative locations of the branch points are controlled primarily by the copolymerization statistics. Several studies that utilize this approach, beginning with the very first report by Kricheldorf,^{5–8} have investigated the effect of branching on various bulk physical properties such as T_g , T_m , crystallinity, etc. More recently, Müller and co-workers⁹ have carried out extensive studies to elucidate the effect of branching density on the solution and melt behavior of hyperbranched polymers prepared using the self-condensing vinyl copolymerization approach. This approach relies on varying the branching density by copolymerization of an inimer with different amounts of a vinyl monomer and, therefore, will possess a similar statistically controlled variation of branch points as in the case of copolycondensation routes. An alternate approach that could provide a greater control over the distribution of branch points would be to incorporate spacer segments of varying lengths directly into the AB_2 -type monomer, which upon self-condensation would generate hyperbranched structures with controllable branching densities. While this approach admittedly

* Corresponding author. E-mail: raman@ipc.iisc.ernet.in.

Scheme 1. Monomer and Polymer Synthesis



cannot access very lightly branched structures, it can provide a very controlled variation within a limited window of branching densities. Very few reports in the literature have utilized this approach for control of branching density.^{10,11} A few years ago, we reported the synthesis of hyperbranched polyurethanes¹² and polyesters,¹³ wherein the primary focus was on the variation of thermal properties as a function of controlled spacer segment length using such an approach.

Recently, we reported the development of a new melt-transetherification route for the preparation of linear polyethers¹⁴ as well as hyperbranched polyethers.¹⁵ Hyperbranched polymers were prepared using an AB₂ monomer based on Mesitol, wherein a monomer precursor **3** (see Scheme 1) was alkylated using 2-chloroethanol to generate the final AB₂ monomer. This precursor **3** is very versatile, in that alkylation using various ω -halo alcohols provides ready access to a range of monomers wherein both the nature and the length of the spacer segment are varied. In the present study, we utilize this strategy to access a wide variety of hyperbranched polyethers that incorporate spacer segments of varying length and flexibility. Various physical attributes, such as the Mark–Houwink exponent “*a*” and *T_g*, have been correlated with the nature and length of spacer segment.

Experimental Section

2,4,6-Trimethylphenol (Mesitol), 2-(2-chloroethoxy)ethanol, 2-[2-(2-chloroethoxy)ethoxy]ethanol, 1,6-hexanediol, 1,8-octanediol, 1,10-decanediol, and camphorsulfonic acid were purchased from Aldrich Chemical Co. 4-Bromobutyl acetate was synthesized from THF using a reported procedure.¹⁶ Structures of all intermediates, monomers, and polymers were confirmed by ¹H NMR spectroscopy. NMR spectra were recorded on a Bruker AV400 MHz spectrometer, using CDCl₃ and TMS as the solvent and reference, respectively. GPC was carried out using Viscotek TDA model 300 system, which coupled with refractive index (RI) and a differential viscometer (DV). The separation was achieved using a series of two PLgel mixed bed columns (300 × 7.5 mm) operated at 30 °C using THF as the eluent. Molecular weights were determined using a universal calibration curve based on the data from the refractive index (RI) and differential viscometric (DV) detectors, using narrow polystyrene standards. The glass transition temperature of the samples was determined using a Rheometric Scientific DSC PLUS instrument at a heating rate of 10 °C/min, under a dry N₂ atmosphere. The samples were first

heated to about 160 °C (to ensure that the sample flows and makes adequate contact with the pan) and quenched prior to recording its *T_g*. The glass transition temperature was taken as the midpoint of the inflection tangent.

3,5-Bis(bromomethyl)-2,4,6-trimethylphenol (2). 50 mL of HBr in acetic acid (33 wt %) was added to the mixture of 4.0 g (2.9 mmol) of mesitol and 2.7 g (2.9 mmol) of trioxane. The mixture was refluxed for 2 h, cooled to RT, and poured into 1.0 L of cold water. The residue was filtered, washed thoroughly with water (4–5 L) to ensure it is acid-free, and then dried under vacuum (yield = 90.0%, mp = 145 °C; lit.¹⁷ 139 °C).

¹H NMR (δ , ppm, CDCl₃): 2.31 (s, 6H, Ar (CH₃)₂); 2.40 (s, 3H, Ar (CH₃)); 4.57 (s, 4H, ArCH₂Br).

3,5-Bis(methoxymethyl)-2,4,6-trimethylphenol (3). Sodium metal (3.2 g, 139.1 mmol) was added to 50 mL of dry methanol in portions. The solution of **2** (7.5 g, 23.3 mmol) in dry methanol (170 mL) was added dropwise to the degassed sodium methoxide solution. The reaction mixture was refluxed for 18 h under a N₂ atmosphere and cooled to room temperature, and the methanol was removed using a rotary evaporator. 80 mL of cold water was added to the residue, and it was acidified with 50% HCl (v/v). The white precipitate formed was extracted with CHCl₃ (120 mL), dried over anhydrous Na₂SO₄, and passed through a silica bed to remove some colored impurities. The chloroform was then removed by a rotary evaporator, and the residue was recrystallized from hot petroleum ether to yield the desired product (yield = 76%, mp = 79 °C; lit. 77–79 °C¹⁵).

¹H NMR (δ , ppm, CDCl₃): 2.25 (s, 6H, Ar(CH₃)₂); 2.35 (s, 3H, Ar(CH₃)); 3.40 (s, 6H, ArCH₂OCH₃); 4.47 (s, 4H, ArCH₂OCH₃); 4.72 (s, 1H, ArOH).

1-(2-Hydroxyethoxy)-3,5-bis(methoxymethyl)-2,4,6-trimethylbenzene (4a; n = 2). A mixture of K₂CO₃ (7.40 g, 53.5 mmol), a catalytic amount of KI, and 2-chloroethanol (1.8 g, 22.3 mmol) were taken in 30 mL of dry CH₃CN. The mixture was degassed for 20 min, after which 2.0 g (8.9 mmol) of **3** was added to it. The reaction mixture was degassed for an additional 20 min and then refluxed for 72 h under a N₂ atmosphere. The solvent was then removed with a rotary evaporator, and 50–60 mL of cold water was added to it. The product was extracted with 100 mL (2 × 50 mL) of ether, and the ether layer was washed with 10% aqueous NaOH solution (4 × 30 mL) followed by water. The ether layer was dried over anhydrous Na₂SO₄ and concentrated, and the residue was recrystallized from hot petroleum ether to give the product (**4a**; n = 2) (yield = 50%; mp = 99–100 °C; lit. 99–100 °C¹⁵).

¹H NMR (δ , ppm, CDCl₃): 2.17 (t, 1H, ArOCH₂CH₂OH); 2.33 (s, 6H, Ar(CH₃)₂); 2.38 (s, 3H, ArCH₃); 3.40 (s, 6H, ArCH₂OCH₃); 3.79 (t, 2H, ArOCH₂CH₂OH); 3.94 (m, 2H, ArOCH₂CH₂OH); 4.47 (s, 4H, ArCH₂OCH₃).

1-(4-Acetoxybutyloxy)-3,5-bis(methoxymethyl)-2,4,6-trimethylbenzene. 3 was coupled with 4-bromobutyl acetate using the above procedure, and the product was purified by distillation using Kugelrohr (220 °C/0.1 mm of Hg) (yield = 82%).

¹H NMR (δ , ppm, CDCl₃): 1.85–1.86 (m, 4H, ArOCH₂-(CH₂)₂CH₂OAc); 2.06 (s, 3H, -OCOCH₃); 2.30 (s, 6H, Ar(CH₃)₂); 2.36 (s, 3H, ArCH₃); 3.38 (s, 6H, ArCH₂OCH₃); 3.65 (t, 2H, Ar-OCH₂-); 4.14 (t, 2H, -CH₂OAc); 4.45 (s, 4H, ArCH₂OCH₃).

1-(4-Hydroxybutoxy)-3,5-bis(methoxymethyl)-2,4,6-trimethylbenzene (4a; n = 4). The above acetate derivative (1.5 g, 4.4 mmol) and 24 mL of 10% aqueous NaOH were refluxed overnight and cooled to RT. The product was extracted into diethyl ether (2 × 30 mL), dried over anhydrous Na₂SO₄, and concentrated. The residue was purified by distillation in the Kugelrohr (240 °C/0.4 mmHg) followed by recrystallization from hot petroleum ether (yield = 75%, mp = 72 °C).

¹H NMR (δ , ppm, CDCl₃): 1.69 (t, 1H, -CH₂OH); 1.78–1.90 (m, 4H, ArOCH₂-(CH₂)₂CH₂OH); 2.30 (s, 6H, Ar(CH₃)₂); 2.36 (s, 3H, ArCH₃); 3.39 (s, 6H, ArCH₂OCH₃); 3.67 (t, 4H, ArOCH₂); 4.14 (m, 2H, CH₂OH); 4.45 (s, 4H, ArCH₂OCH₃).

1-(ω -Hydroxyalkyloxy)-3,5-bis(methoxymethyl)-2,4,6-trimethylbenzene (4a; n = 6–10). **3** was coupled with the

appropriate ω -bromoalkanol using the same procedure as above, and the product was purified by distillation using a Kugelrohr followed by recrystallization from petroleum ether. The yields and NMR data are provided below.

4a; $n = 6$; yield = 73%, mp = 73 °C: ^1H NMR (δ , ppm, CDCl_3): 1.40–1.85 (m, 8H, $\text{ArOCH}_2(\text{CH}_2)_4\text{CH}_2\text{OH}$); 2.30 (s, 6H, $\text{Ar}(\text{CH}_3)_2$); 2.36 (s, 3H, $\text{Ar}(\text{CH}_3)$); 3.38 (s, 6H, $\text{ArCH}_2\text{OCH}_3$); 3.61–3.63 (m, 4H $\text{ArOCH}_2(\text{CH}_2)_4\text{CH}_2\text{OH}$); 4.45 (s, 4H, $\text{ArCH}_2\text{OCH}_3$).

4a; $n = 8$; yield = 70%, mp = 70 °C: ^1H NMR (δ , ppm, CDCl_3): 1.37–1.81 (m, 12H, $\text{ArOCH}_2(\text{CH}_2)_6\text{CH}_2\text{OH}$); 2.30 (s, 6H, $\text{Ar}(\text{CH}_3)_2$); 2.36 (s, 3H, $\text{Ar}(\text{CH}_3)$); 3.38 (s, 6H, $\text{ArCH}_2\text{OCH}_3$); 3.61–3.63 (m, 4H, $\text{ArOCH}_2(\text{CH}_2)_6\text{CH}_2\text{OH}$); 4.46 (s, 4H, $\text{ArCH}_2\text{OCH}_3$).

4a; $n = 10$; yield = 70%, mp = 75 °C: ^1H NMR (δ , ppm, CDCl_3): 1.37–1.81 (m, 14H, $\text{ArOCH}_2(\text{CH}_2)_7\text{CH}_2\text{OH}$); 2.30 (s, 6H, $\text{Ar}(\text{CH}_3)_2$); 2.36 (s, 3H, $\text{Ar}(\text{CH}_3)$); 3.38 (s, 6H, $\text{ArCH}_2\text{OCH}_3$); 3.61–3.63 (m, 4H, $\text{ArOCH}_2(\text{CH}_2)_7\text{CH}_2\text{OH}$); 4.46 (s, 4H, $\text{ArCH}_2\text{OCH}_3$).

1-(ω -Hydroxyoligoethyleneoxy)-3,5-bis(methoxymethyl)-2,4,6-trimethylbenzene (4b, $n = 2$ or 3). **3** was coupled with 2-(2-chloroethoxy)ethanol (or 2-[2-(2-chloroethoxy)ethoxy]ethanol) using the same procedure as for the alkylene series (**4a**).

4b, $n = 2$; yield = 50%: ^1H NMR (δ , ppm, CDCl_3): 2.33 (s, 6H, $\text{Ar}(\text{CH}_3)_2$); 2.37 (s, 3H, $\text{Ar}(\text{CH}_3)$); 3.40 (s, 6H, $\text{ArCH}_2\text{OCH}_3$); 3.63–3.85 (m, 8H, $\text{ArOCH}_2\text{CH}_2\text{OCH}_2\text{CH}_2\text{OH}$); 4.46 (s, 4H, $\text{ArCH}_2\text{OCH}_3$).

4b, $n = 3$; yield = 50%: ^1H NMR (δ , ppm, CDCl_3): 2.33 (s, 6H, $\text{Ar}(\text{CH}_3)_2$); 2.37 (s, 3H, $\text{Ar}(\text{CH}_3)$); 3.40 (s, 6H, $\text{ArCH}_2\text{OCH}_3$); 3.63–3.85 (m, 12H, $\text{ArOCH}_2\text{CH}_2\text{OCH}_2\text{CH}_2\text{OCH}_2\text{CH}_2\text{OH}$); 4.46 (s, 4H, $\text{ArCH}_2\text{OCH}_3$).

1-(4-Hydroxymethylcyclohexylmethoxy)-3,5-bis(methoxymethyl)-2,4,6-trimethylbenzene (4c). **3** was coupled with 4-bromomethylcyclohexylmethanol using the same procedure as for the alkylene series (**4a**), and the product was purified by recrystallization from hot petroleum ether (yield = 52%, mp = 110–111 °C).

^1H NMR (δ , ppm, CDCl_3): 0.9–2.0 (m, 10H, cyclohexane); 2.30 (s, 6H, $\text{Ar}(\text{CH}_3)_2$); 2.37 (s, 3H, $\text{Ar}(\text{CH}_3)$); 3.39 (s, 6H, $\text{ArCH}_2\text{OCH}_3$); 3.44–3.49 (m, 4H, CH_2 -cyclohexyl); 4.46 (s, 4H, $\text{ArCH}_2\text{OCH}_3$).

Typical Polymerization Procedure. 1-(2-Hydroxyethoxy)-3,5-bis(methoxymethyl)-2,4,6-trimethylbenzene **4a** ($n = 2$) (600 mg, 2.2 mmol) along with 2 mol % of pyridinium camphor sulfonate (PCS) was placed in the test tube-shaped polymerization tube. It was degassed for 10 min and dipped into an oil bath at 110 °C under continuous N_2 purge, to ensure homogeneous mixing of catalyst with monomer. The temperature of the oil bath was raised to 150 °C, and polymerization was carried out under N_2 for 2 h with constant stirring. The polymerization tube was cooled to room temperature and connected to a Kugelrohr apparatus, in which the polymerization was continued for an additional 1 h at 150 °C under reduced pressure (0.1 Torr), with continuous mixing of the melt by rotation. The polymer was dissolved in THF, and the solution was neutralized with solid NaHCO_3 and filtered. The filtrate was concentrated and poured into methanol to obtained polymer. All polymers were purified further by dissolution followed by reprecipitation. Typical yields of the purified polymer ranged from 50 to 60%.

Results and Discussion

Polymer Synthesis. Using mesitol as the starting material, monomer **3** was prepared in two steps involving a high yielding bis(bromomethylation) step followed by transformation of the bromomethyl groups to methoxymethyl groups (Scheme 1).¹⁸ The controlled variation of the spacer segment in the hyperbranched structures was affected by incorporation of the spacer into the AB_2 -type monomer at this stage. A series of monomers containing alkylene spacers (**4a**) of varying lengths, from C2 to C10, were prepared by coupling **3** with the

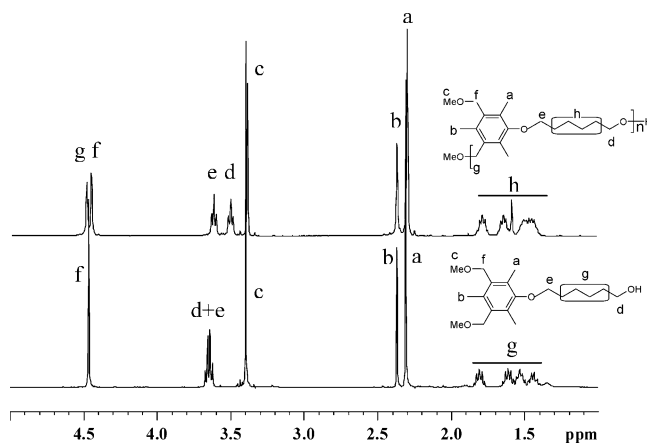


Figure 1. ^1H NMR spectra of a representative monomer **4a** ($n = 6$) and the corresponding polymer **HP-C6**.

required ω -bromoalkanol. Similarly, a series of monomers with relatively flexible oligo-oxyethylene spacers (**4b**) and one with a stiff cycloalkylene spacer (**4c**) were also prepared. The structures of all the monomers were confirmed by their ^1H NMR spectra.¹⁹

Polymerization of the various AB_2 monomers proceeded under acid-catalyzed transesterification conditions, with the exclusion of methanol, to yield hyperbranched polyethers with fairly high molecular weights. The transesterification process occurs readily because of the ease of formation of the benzylic carbocationic intermediate during the acid-catalyzed process. The three methyl groups on the benzene ring of the monomer are essential to prevent cross-linking that can occur via an electrophilic aromatic substitution.¹⁵ An improved catalyst, namely pyridinium camphor sulfonate (PCS), was used to affect the polycondensation, as the polymerization under these conditions proceeded cleanly with fewer side reactions.²⁰ Furthermore, the direct polymerization of **3**, which had failed to give the desired polymer using PTSA as the catalyst, gave a soluble polymer **HP-C0** with the expected structure using PCS as the catalyst. In Figure 1, we compare the spectra of one representative monomer **4a** ($n = 6$) with that of the corresponding polymer **HP-C6**. Upon polymerization the benzylic protons peaks (~ 4.5 ppm) split into two peaks of equal intensity: one belonging to CH_3OCH_2 — and the other to $-\text{R}-\text{OCH}_2-$, which suggests that the extent of conversion is fairly high leading to the loss of one of the methoxy groups in the form of methanol.

Furthermore, the coincidental overlap of the $\text{Ar}-\text{O}-\text{CH}_2-$ and the $-\text{CH}_2\text{OH}$ protons (~ 3.6 – 3.7 ppm) in this monomer is lifted upon polymerization, and the two types of alkoxymethyl protons appear as two separate triplets of equal intensity. The relative intensities of all the other proton signals conform to the expected polymer structure.

The ^1H NMR spectra of the various other hyperbranched polymers are compared in Figure 2. In most cases, one sees two sets of triplets in the region between 3.5 and 4.0 ppm, corresponding to the two types of alkoxymethylene protons of the spacer. Furthermore, in the case of the alkylene series the difference between the two types of benzylic protons (in the 4.5 ppm region), which is very significant in the **HP-C2** case, decreases considerably as the spacer length increases. The presence of a β -oxygen atom in the **HP-C2** case causes this large difference. In the case of the oligo-oxyethylene series, however, the difference between these two peaks

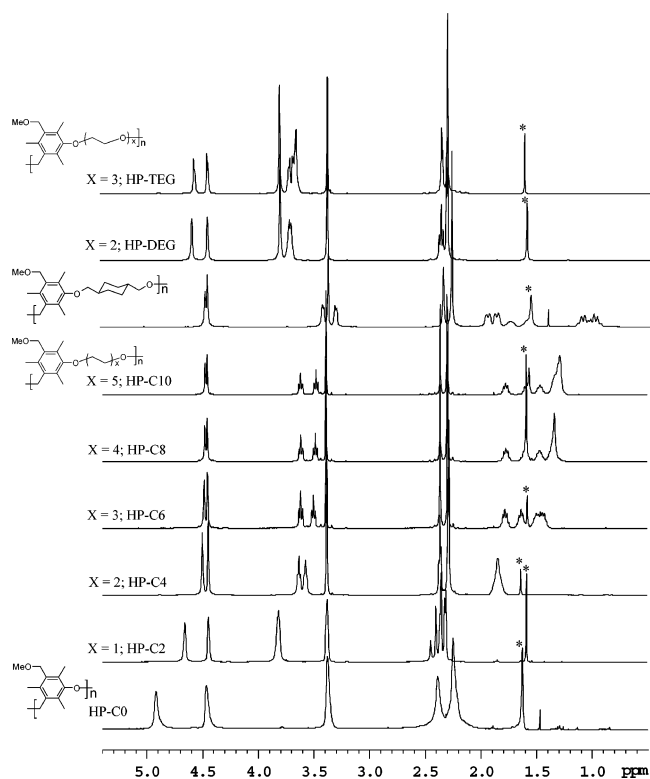


Figure 2. ^1H NMR spectra of the various hyperbranched polymers. The peak indicated by an asterisk is due to water.

reduces only slightly (as the β -oxygen atom is always present), and it is roughly the same in cases of **HP-DEG** and **HP-TEG**. Apart from these differences, the ability to discriminate between the dendritic and linear defect units, which was possible in the case of **HP-C2** utilizing the multiplicity of the aromatic methyl protons signals (~ 2.2 – 2.5 ppm),¹⁵ is lost because these protons become less sensitive to the different types of environments present in polymers having longer spacer segments. In all the polymers belonging to the alkylene spacer series, essentially only two peaks (with intensity ratio of 1:2) are seen (some weak shoulders are visible in the spectra of **HP-C4**), confirming the complete loss of sensitivity to the presence of defect units. In the case of **HP-DEG** some splitting remains, although the assignments were difficult to make. Hence, the degree of branching (DB) in most of these polymers was difficult to establish. Quite unexpectedly, even in the case of the polymer without a spacer, **HP-C0**, only two types of methyl protons are seen, suggesting that the structure/conformation of **HP-C2** appears to specifically enable the discrimination of the different types of subunits. The spectrum of the polymer with a cyclohexanedimethylene spacer (**HP-CDM**) also exhibited a similar pattern in the aromatic methyl region, leaving little possibility of determining the degree of branching. In the case of this polymer, the spacer segment contains both the cis and trans forms in the ratio 20:80,²¹ although in the polymer the peaks due to these isomers were not resolvable.

Molecular Weights and Conformational Characteristics. The molecular weights of the polymers were determined by GPC at 30 °C in THF, using a dual detector system, consisting of a refractive index (RI) and a differential viscometric (DV) detector connected in series. The molecular weights of all the polymers were determined by the universal calibration method and were found to be reasonably high, with M_w values

Table 1. Various Physical Attributes of the Different Hyperbranched Polymers

polymer	M_w	PDI	α^a	T_g (°C)
HP-C0	24 000	1.7	0.370	88
HP-C2	83 000	3.9	0.399	36
HP-C4	53 200	3.0	0.405	12
HP-C6	51 100	2.5	0.449	1
HP-C8	59 900	2.7	0.477	−8
HP-C10	38 300	1.6	0.540	−18
HP-DEG	90 000	1.9	0.426	−3
HP-TEG	70 300	1.7	0.459	−16
HP-CDM	28 300	2.1	0.430	77

^a Mark–Howink exponent determined by GPC in THF at 30 °C using a dual detector setup.

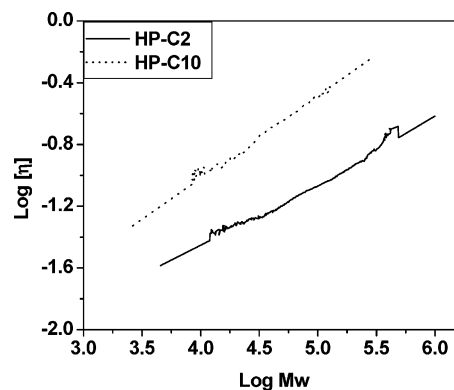


Figure 3. Mark–Howink plots of two representative hyperbranched polymers obtained using the GPC equipped with a dual detector.

ranging from 24 000 to 90 000, as seen in Table 1. Inclusion of spacer segments of various lengths into the monomer structure makes it possible to vary the distance between the branch points in the hyperbranched polymer in a controlled fashion, thereby permitting one to probe the effect of such a variation on the conformational properties of the hyperbranched polymer. This analysis, of course, assumes that the degree of branching in these polymers is invariant with spacer segment length. We make this assumption, first, because it is difficult to directly determine the DB, and second, we feel that there are no compelling factors that should cause deviations from the statistically controlled degree of branching with increasing spacer segment length.²² The use of the dual detector system permitted the determination of the Mark–Howink exponents for the various hyperbranched polymers. Typically, the DV detector directly measures the intrinsic viscosities of the various slices of each chromatogram (done in THF at 30 °C), while the RI detector measures their concentrations.

Using a universal calibration plot based on polystyrene standards, the M_w values for each slice are determined, from which the M–H plots (Figure 3) are constructed. It is apparent that, unlike in the case of dendrimers,²³ the intrinsic viscosity does not go through a maximum in such a plot, reaffirming that the degree of branching in these systems are not very high, as is the case with typical hyperbranched polymers. Computational studies by Lyulin et al. have suggested that such a maximum in intrinsic viscosity would be seen only when the degree of branching exceeds 0.8.²⁴ Experimental studies of hyperbranched polymers have also confirmed the linear variation of the intrinsic viscosity with molecular weight.²⁵ The M–H exponent “ α ”, which is a measure of the relative compactness of

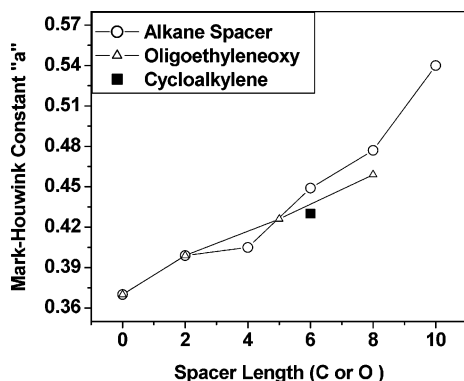


Figure 4. Variation of the Mark-Houwink exponent " a " of the various hyperbranched polymers as a function of the number of atoms in the spacer segment.

the polymer chain, is plotted as a function of spacer length in Figure 4. The a value for the parent hyperbranched polymer **HP-C0** without a spacer is 0.37, and it increases gradually to 0.54 for **HP-C10**. A similar increase in the a value with spacer length is also seen in the case of the relatively more flexible oligo-oxyethylene spacers, although the extent of increase in these systems (considering the same number of atoms in the spacer segment) appears to be slightly smaller. Interestingly, the a value for the relatively more rigid polymer, **HP-CDM**, is also slightly lower than what might be expected for a C6 spacer length. These observations confirm that as the length of the spacer between branching points decreases, i.e., when the branching density increases, the compactness of the hyperbranched polymers increases. They are also in concurrence with the expectation that at the limits of very low branching density (per unit volume), i.e., in the presence of very long spacers, the polymers will behave more like linear analogues. Studies by Müller and co-workers,⁹ using randomly branched hyperbranched polyacrylates, however, appear to suggest that fairly compact structures are formed even in the presence of very low levels of a branching agent, namely the inimer. Their studies using the copolymerization of simple acrylates with specifically designed inimers, it appears, could generate systems that are considerably different from those presented in this study, where the hyperbranched polymers are prepared via the simple AB_2 self-condensation approach.²⁶ Similar studies were also reported by Weimer et al.,²⁷ using self-condensation vinyl copolymerizations.

Another aspect that is of interest is the effect of molecular weight on the compactness of hyperbranched structures. In perfect dendrimers, it has been shown that spherical compact structures are formed only at higher generations, i.e., at higher molecular weights.²⁸ It may be expected that even in hyperbranched structures this will be true although they possess no specific core or discrete generations. To understand the effect of molecular weight on the compactness of hyperbranched structures, we fractionated two polymers, **HP-C2** and **HP-C10**, which represent polymers with distinctly different branching densities. Typical GPC profiles of the fractionated samples of **HP-C2** are shown in Figure 5. It is apparent that the lower molecular weight fractions are fairly monodisperse, but the distribution becomes broader for the higher molecular weight fractions, possibly reflecting an intrinsic constraint of the fractionation process.²⁹ To confirm that the branching density is invariant with molecular weight, the NMR

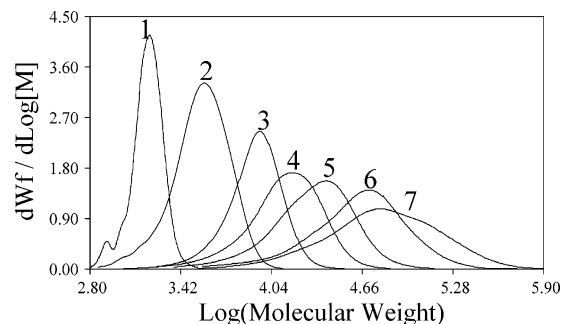


Figure 5. GPC elution profiles of various fractionated samples of **HP-C2**.

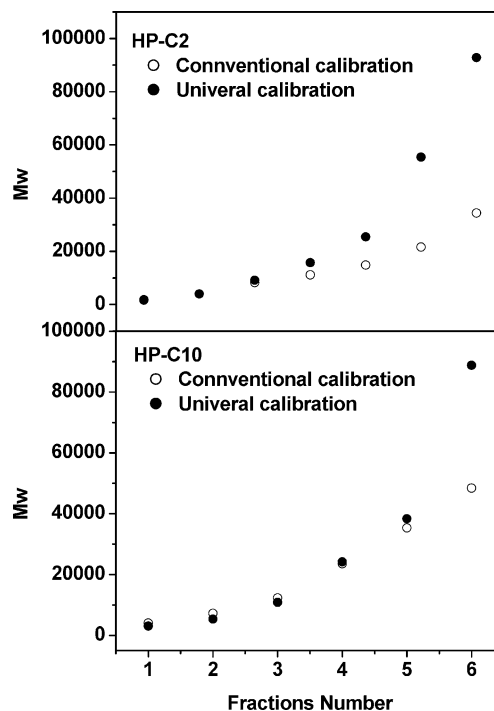


Figure 6. Comparison of molecular weights determined by the standard PS calibration with those determined by the universal calibration plot.

spectra of a few representative fractions were recorded and shown to be essentially identical.³⁰ The use of the dual detector system to determine the $M-H$ exponents requires samples that are polydisperse ($PDI \sim 2$), which is essential for adequate molecular weight sampling during the elution. Therefore, the a values could not be accurately determined for the fractionated samples, and hence, we chose to compare the molecular weights of the fractionated samples obtained using the standard calibration (using PS standards) with those obtained from the universal calibration plot. The difference between these two values is a reflection of the compactness of the structure; the more compact the structure, the greater is the extent of underestimation using the standard calibration plot. A plot of the molecular weights of the various fractions determined using both these calibrations is shown in Figure 6. In the case of the more densely branched **HP-C2** polymer, it is clear that the extent of underestimation increases with the molecular weight and becomes significant only above molecular weights of about 10 000. The extent of this underestimation is fairly large for the highest molecular weight fraction; the molecular weight using PS calibration is almost a third of the actual one. Furthermore, the change is fairly discontinuous, as was reported in

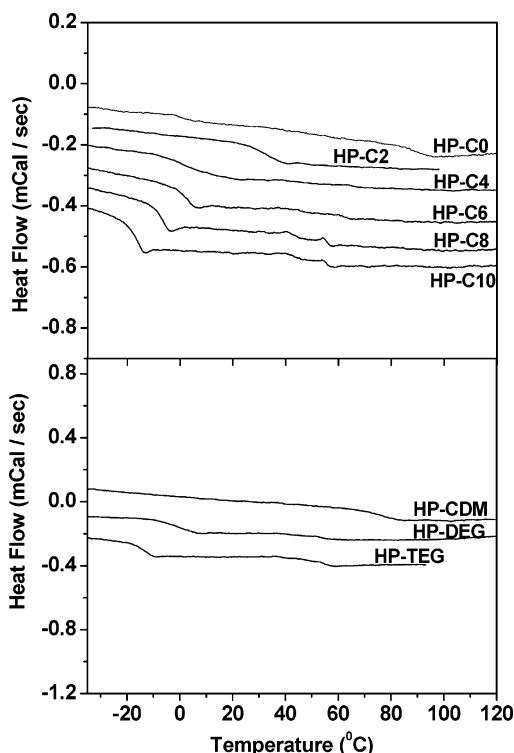


Figure 7. DSC thermograms of the hyperbranched polymers. A weak T_g -like transition is seen in some cases at around 50–60 °C, whose origin is still unclear.

the case of dendrimers,²⁸ where it was seen that a sudden change in the compactness occurs for the fifth-generation polymers ($M_n \sim 6700$) when compared to their linear analogues. In contrast, in the case of the **HP-C10** polymer, which has a much lower density of branching, the extent of underestimation becomes significant only at much higher molecular weights ($\sim 35\,000$) and is fairly large for the highest molecular weight fraction (roughly $1/2$).

This difference in behavior between the densely branched and lightly branched systems is in general agreement with the observation that the **HP-C10** has a significantly higher α value when compared to that of **HP-C2**. A similar inference can also be drawn from some of the results presented by Simon et al.,³¹ where the contraction factor g' ($\eta_{\text{branched}}/\eta_{\text{linear}}$) appears to reach the limiting value of 1 (which corresponds to linear systems) at relatively higher molecular weights for polymers with lower branching density. One aspect of practical importance that emerges from these plots is that the use of a standard GPC setup can lead to seriously underestimated molecular weights in hyperbranched polymers, and more importantly, the extent of this underestimation becomes larger for higher molecular weight samples, as was previously shown by Gitsov et al.³² in linear–dendritic hybrid systems.

Thermal Analysis. To elucidate the effect of spacer segment length on the T_g , the DSC thermograms of the all polymers were recorded (Figure 7). The T_g 's of the hyperbranched polymers were seen to decrease monotonically with increasing spacer segment length. A plot depicting this variation as a function of the number of atoms in the spacer segment (Figure 8) permits the direct comparison of the alkylene spacer with those having oligo-oxyethylene ones. It is clear that, as expected, the polymers belonging to the latter series have significantly lower T_g values reflecting their higher

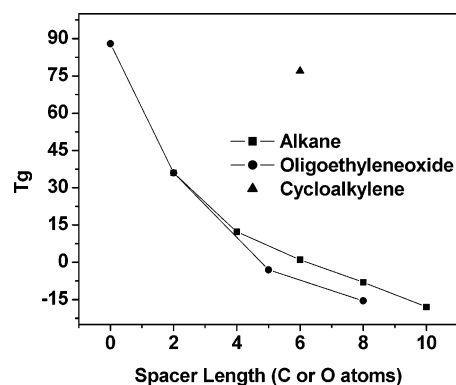


Figure 8. Variation of T_g of hyperbranched polymers as a function of spacer segment length and flexibility.

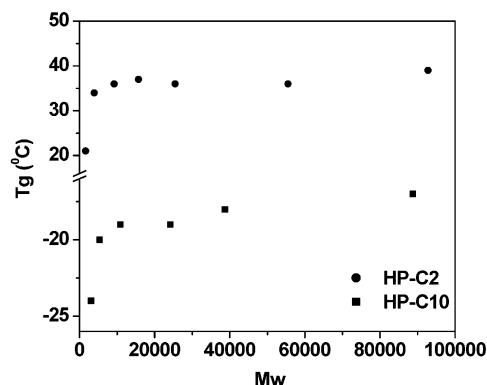


Figure 9. Variation of T_g as a function of molecular weight.

flexibility. A similar decrease of T_g with spacer segment length was earlier reported by us in the case of polyesters¹² and polyurethanes.¹³ The polymer **HP-CDM**, on the other hand, has a significantly higher T_g (compared to that of the C-6 spacer) due to the rigid nature of the cycloaliphatic spacer segment. The T_g of the parent hyperbranched polymer **HP-C0** without a spacer is also high, around 88 °C.³³

The T_g 's of all the fractionated samples (of both **HP-C2** and **HP-C10**) were also determined, and the variation of T_g as a function of molecular weight is plotted in Figure 9. In both cases, one sees the expected steep dependence at lower molecular weights with a leveling off at higher molecular weights. This is consistent with earlier observations on hyperbranched polyesters of varying molecular weights made by Parker and Feast,³⁴ although the molecular weights at which the leveling is observed in our system is somewhat lower. Similar variation of T_g with generation was observed in the case of dendrimers, where the T_g was seen to level off after the fourth generation.³⁵ It is also interesting to note here that the absolute magnitude of the change is significantly larger for the densely branched (more stiffer) system (**HP-C2**) than for the **HP-C10**. Stutz made a similar observation when comparing dendrimers having different backbone structures, wherein a steeper dependence of T_g with generation was seen in systems where the T_g of the parent linear backbone is higher.³⁶

Conclusions

A series of hyperbranched polyethers containing spacer segments of varying nature and length were prepared via a melt-transesterification polycondensation process. The synthesis was achieved using a single AB_2 -type monomer intermediate, which directly incor-

porated the different spacers. The structures of the monomers and the polymers were confirmed by their ^1H NMR spectra. The molecular weights of the polymers were determined by GPC using the universal calibration method and were found to be fairly high. From the variation of the Mark–Howink constants “ a ”, which were determined using a GPC system equipped with a dual detector (RI-DV) system, it was shown that the relative compactness of hyperbranched polymers decreases with increasing length of the spacer segment; i.e., more densely branched polymers form more compact structures. This is the first study wherein the compactness of hyperbranched polymers has been examined by systematically varying the length of the spacer segment in the AB_2 monomer.

Furthermore, GPC studies of a series of fractionated samples of **HP-C2** and **HP-C10** revealed that, as in the case of dendrimers, relatively compact conformations are adopted by hyperbranched polymers only when their molecular weights are above a certain threshold value. Importantly, it was also noticed that in densely branched **HP-C2**, compact structures are formed at relatively lower molecular weights when compared to lightly branched **HP-C10**. Finally, it was shown that the T_g of hyperbranched polymers depends on both the length and flexibility of the spacer segment—the T_g of hyperbranched polymers decreased monotonically with increasing spacer length, and as expected, polymers with relatively flexible spacers have lower T_g than ones with relatively rigid ones. The variation of T_g as a function of molecular weight was investigated in both the lightly and densely branched systems and was seen to exhibited the expected rapid increase followed by a leveling off at higher molecular weights. Interestingly, the relatively stiffer (densely branched) **HP-C2** polymer showed a larger variation in T_g than the more flexible **HP-C10** system.

Acknowledgment. We thank the Department of Science and Technology, New Delhi, for their generous funding (SP/S-1/G07/99) and 3M-India Ltd. for the Research Award to our laboratory.

Supporting Information Available: NMR spectra of all monomers, the representative fractions of the hyperbranched polymer **HP-C2**, molecular weights of each fractions of both **HP-C2** and **HP-C10**, and GPC elution profiles of various fractionated samples of **HP-C10**. This material is available free of charge via the Internet at <http://pubs.acs.org>.

References and Notes

- (1) For recent reviews on hyperbranched polymers see: (a) Gao, C.; Yan, D. *Prog. Polym. Sci.* **2004**, *29*, 183. (b) Mori, H.; Muller, A. H. E. *Top. Curr. Chem.* **2003**, *228*, 1. (c) Voit, B. *J. Polym. Sci., Part A: Polym. Chem.* **2000**, *38*, 2505. (d) Burchard, W. *Adv. Polym. Sci.* **1999**, *143*, 113. (e) Hawker, C. J. *Adv. Polym. Sci.* **1999**, *147*, 113. (f) Hult, A.; Johansson, M.; Malmstrom, E. *Adv. Polym. Sci.* **1999**, *143*, 1.
- (2) (a) Yan, D.; Gao, C. *Macromolecules* **2000**, *33*, 7693. (b) Gao, C.; Yan, D. *Chem. Commun.* **2001**, 107. (c) Jikie, M.; Chon, S. H.; Kakimoto, M.; Kawauchi, S.; Imase, T.; Watanabe, J. *Macromolecules* **1999**, *32*, 2061. (d) Emrick, T.; Chang, H. T.; Fréchet, J. M. J. *Macromolecules* **1999**, *32*, 6380.
- (3) Fréchet, J. M. J.; Henmi, H.; Gitsov, I.; Aoshima, S.; Leduc, M.; Grubbs, R. B. *Science* **1995**, *269*, 1080.
- (4) Chang, H. T.; Fréchet, J. M. J. *J. Am. Chem. Soc.* **1999**, *121*, 2313.
- (5) Kricheldorf, H. R.; Zang, Q. Z.; Schwarz, G. *Polymer* **1982**, *23*, 1821. Kricheldorf, H. R.; Stober, O.; Lubbers, D. *Macromol. Chem. Phys.* **1995**, *196*, 3549. Kricheldorf, H. R.; Stukenbrock, T. *Polymer* **1997**, *38*, 3373. Kricheldorf, H. R.; Stukenbrock, T. *J. Polym. Sci., Part A: Polym. Chem.* **1998**, *36*, 2347.
- (6) Jayakannan, M.; Ramakrishnan, S. *J. Polym. Sci., Polym. Chem. Ed.* **1998**, *36*, 309. Jayakannan, M.; Ramakrishnan, S. *J. Polym. Sci., Polym. Chem. Ed.* **2000**, *38*, 261.
- (7) Kunamane, S.; Buzza, D. M. A.; Parker, D.; Feast, W. J. *J. Mater. Chem.* **2003**, *13*, 2749.
- (8) Frey, H.; Höltel, D. *Acta Polym.* **1999**, *50*, 67. Mock, A.; Burgath, A.; Hanselmann, R.; Frey, H. *Polym. Mater. Sci. Eng.* **1999**, *80*, 173.
- (9) (a) Simon, P. F. W.; Muller, A. H. E.; Pakula, T. *Macromolecules* **2001**, *34*, 1677. (b) Simon, P. F. W.; Muller, A. H. E. *Macromolecules* **2001**, *34*, 6206.
- (10) Hawker, C. J.; Chu, F.; Pomery, P. J.; Hill, D. J. T. *Macromolecules* **1996**, *29*, 3831.
- (11) Suneel, Buzaa, D. M. A.; Groves, D. J.; McLeish, T. C. B.; Parker, D.; Keeney, A. J.; Feast, W. J. *Macromolecules* **2002**, *35*, 9605.
- (12) Kumar, A.; Ramakrishnan, S. *J. Polym. Sci., Part A: Polym. Chem.* **1996**, *34*, 839.
- (13) Kumar, A.; Ramakrishnan, S. *Macromolecules* **1996**, *29*, 2524.
- (14) Jayakannan, M.; Ramakrishnan, S. *Macromol. Chem. Phys.* **2000**, *201*, 759.
- (15) Jayakannan, M.; Ramakrishnan, S. *Chem. Commun.* **2000**, 1967.
- (16) Goldsmith, D. J.; Kennedy, E.; Campbell, R. G. *J. Org. Chem.* **1975**, *40*, 3571.
- (17) Bodwell, G. J.; Bridson, J. N.; Chen, S.; Poirier, R. A. *J. Am. Chem. Soc.* **2001**, *123*, 4704.
- (18) The bromomethylation approach was a significant improvement over our previous chloromethylation one,¹⁵ in terms of improved yield as well as its facileness.
- (19) The proton NMR spectra of all the monomers are available in the Supporting Information.
- (20) Behera, G. C.; Ramakrishnan, S. *J. Polym. Sci., Part A: Polym. Chem.* **2004**, *42*, 102.
- (21) This value was determined for the starting cyclohexanedimethanol and is assumed to be the same in the case of the polymer.
- (22) The extent of cyclization could increase with increasing spacer length and flexibility. Since topological constraints in hyperbranched structures impose a maximum of one cyclization per polymer molecule, its effect on the chain conformation might be expected to be very limited.
- (23) Mourey, T. H.; Turner, S. R.; Rubinstien, M.; Fréchet, J. M. J. *Macromolecules* **1992**, *25*, 2401. Hawker, C. J.; Farrington, P. J.; Mackay, M. E.; Wooley, K. L. Fréchet, J. M. J. *J. Am. Chem. Soc.* **1995**, *117*, 4409.
- (24) Lyulin, A. V.; Adolf, D. B.; Davies, G. R. *Macromolecules* **2001**, *34*, 3783.
- (25) Turner, S. R.; Voit, B. I.; Mourey, T. H. *Macromolecules* **1993**, *26*, 4617. Turner, S. R.; Walter, F. Voit, B. I.; Mourey, T. H. *Macromolecules* **1994**, *27*, 1611.
- (26) Yan et al. ascribe the difference in behavior to the different reactivities of the propagating and initiating centers during polymer growth, which renders the simple statistical analysis of degree of branching inapplicable. Yan, D.; Muller, A. H. E.; Matyjaszewski, K. *Macromolecules* **1997**, *30*, 7024.
- (27) Weimer, M. W.; Fréchet, J. M. J.; Gitsov, I. *J. Polym. Sci., Part A: Polym. Chem.* **1998**, *36*, 955.
- (28) Hawker, C. J.; Malmström, E. E.; Frank, C. W.; Kampf, J. P. *J. Am. Chem. Soc.* **1997**, *119*, 9903.
- (29) The molecular weights and PDI's of various fractionated samples are tabulated in the Supporting Information.
- (30) In the case of **HP-C2**, wherein the DB is reflected in the aromatic methyl region, one sees little change in the relative intensities of the various peaks for different molecular weight fractions. The NMR spectra of three representative fractions are available in the Supporting Information.
- (31) See Figure 5 in ref 9b.
- (32) Gitsov, I.; Fréchet, J. M. J. *Macromolecules* **1994**, *27*, 7309.
- (33) A structurally similar hyperbranched poly(benzyl ether) (devoid of the aromatic methyl groups) reported by Uhrich et al. having phenolic end groups (prepared via an A_2B monomer) exhibited a surprisingly low T_g value of only ca. 30 °C.
- (34) Parker, D.; Feast, J. W. *Macromolecules* **2001**, *34*, 2048.
- (35) Wooley, K. L.; Hawker, C. J.; Pochan, J. M.; Fréchet, J. M. J. *Macromolecules* **1993**, *26*, 1514.
- (36) Stutz, H. *J. Polym. Sci., Part B: Polym. Phys.* **1995**, *33*, 333.